Transient transfection of mammalian cells using a violet diode laser

Maria Leilani Torres-Mapa
University of St. Andrews
Scottish University Physics Alliance (SUPA)
School of Physics and Astronomy
North Haugh
St. Andrews KY16 9SS, Scotland
United Kingdom

Liselotte Angus
University of St. Andrews
School of Biology
Fife, St. Andrews
KY16 9TS, Scotland
United Kingdom

Martin Ploschner
Kishan Dholakia*
University of St. Andrews
Scottish University Physics Alliance (SUPA)
School of Physics and Astronomy
North Haugh
St. Andrews KY16 9SS, Scotland
United Kingdom

Frank J. Gunn-Moore*
University of St. Andrews
School of Biology
Fife, St. Andrews
KY16 9TS, Scotland
United Kingdom

Abstract. We demonstrate the first use of the violet diode laser for transient mammalian cell transfection. In contrast to previous studies, which showed the generation of stable cell lines over a few weeks, we develop a methodology to transiently transfect cells with an efficiency of up to ~40%. Chinese hamster ovary (CHO-K1) and human embryonic kidney (HEK293) cells are exposed to a tightly focused 405-nm laser in the presence of plasmid DNA encoding for a mitochondrial targeted red fluorescent protein. We report transfection efficiencies as a function of laser power and exposure time for our system. We also show, for the first time, that a continuous wave laser source can be successfully applied to selective gene silencing experiments using small interfering RNA. This work is a major step towards an inexpensive and portable phototransfection system. [DOI: 10.1117/1.3430730]

Keywords: photoporation; phototransfection; gene transfection; gene knockdown; violet diode.

Paper 09428SSR received Sep. 22, 2009; revised manuscript received Dec. 18, 2009; accepted for publication Dec. 29, 2009; published online Jul. 7, 2010.

1 Introduction

Photoporation refers to the use of tightly focused laser light to perforate temporarily the cellular membrane and allow exogenous material to be taken up by the cell.[1] This technique has become increasingly popular due to its simplicity, robustness, and efficiency. Most of its applications have been predominantly, but not limited to, the delivery of nucleic acids such as plasmid DNA[1–3] and messenger RNA[4] to intracellular compartments. In addition, dyes,[2] nanoparticles,[5] and semiconductor nanocrystals[6] can also be injected into the cells, which can be useful for monitoring gene or, potentially, drug activity.

Various laser-based systems have been used for photoporation and ultimately cell transfection. Wavelengths in the ultraviolet[7] (UV), visible[1,6,8–10] (VIS), and infrared[2–4,11] (IR), in both pulsed (nanosecond or femtosecond) and continuous wave (cw) mode, have all been used for cell transfection. The mechanism for poration is dependent on the type of laser used and its pulse duration.[12] Femtosecond cell transfection has currently emerged as the most ubiquitous and consistent method, but this system requires the use of expensive lasers with a typically large footprint (e.g., the ti-sapphire femtosecond laser oscillator). In terms of cw lasers in the VIS light region, the first laser used for cell transfection was the 488-nm output line of an argon-ion laser, which again has a large footprint.[8] In 2005, Paterson et al. used a low-cost cw violet diode laser for cell transfection, which is currently the simplest and most inexpensive method of laser-mediated transfection.[1] They showed that with sufficient control of laser parameters, cw VIS lasers are as effective as their femtosecond IR counterparts. Optical power densities as low as ~1200 MW/m^2 have been successfully used for such cell photoporation.[1] Crucially for the purposes of our discussion, previous studies with the violet diode did not achieve transient transfection but only stable transfection due to the limited material they could deliver to the cell. In stable transfection, only cells that have integrated the plasmid DNA into the cell's genetic genome are selected, and such stable cell lines take many weeks to generate. Transient transfection, as opposed to stable transfection, relies on the transcription and translation of the plasmid DNA itself, and this only takes 24 to 72 h to be achieved; such an inexpensive transient

*Contributed equally to this work.
Address all correspondence to: Maria Leilani Torres-Mapa, University of St. Andrews, Scottish University Physics Alliance (SUPA), School of Physics and Astronomy, North Haugh, St. Andrews, Fife, KY169SS, Scotland, United Kingdom. Tel: 44-1334-461654; Fax: 44-1334-463104; E-mail: mlt9@st-andrews.ac.uk

1083-3668/2010/15(4)/041506/7/$25.00 © 2010 SPIE

method for protein and drug delivery would be of great interest, especially for clinical applications.

Diode lasers are inexpensive and offer a compact footprint, important for miniaturization and automation. Notably, diode lasers at violet-blue wavelengths are already incorporated into most confocal microscope systems and fluorescence-activated cell sorting (FACS) machines. It is thought that the mechanism of photopore generation by cw irradiation relies on the cumulative temperature increase that occurs within a few milliseconds to alter the permeability of the cell.[8,10] An absorptive chemical species in the violet-blue region, such as phenol red dye, is used to aid absorption and local increase in temperature.[8–10] The advantage of using this dye is that it is nontoxic, is easily removed by washing, and is ubiquitously used in cell culture medium.

In this paper, we demonstrate for the first time the successful use of violet diode lasers for transient transfection of mammalian cell lines including the Chinese hamster ovary (CHO-K1) and human embryonic kidney (HEK293) lines. Previously, VIS wavelength cw lasers were shown to transfect CHO-K1,[1,10] NIH3T3 murine fibroblast,[8] and human cardiac cells.[9] Each cell line, due to its differing chemical functions and properties can have diverse reactions to irradiation from a given laser. Here, we show that we can repeatedly and robustly transfect mammalian cell lines using this system with an efficiency of up to ~40%. Additionally, previous reports using a cw 488-nm argon ion laser explored only a single optical power density.[8–10] In contrast, in this study we varied the optical power density and exposure time to determine the optimal parameters for cw transfection. In conjunction with this work, we performed an extensive study on cell viability by varying exposure times for two laser powers to elucidate its effect on cell death and poration. Furthermore, we also propose the use of this violet diode system as an inexpensive tool for specific gene knockdown experiments. To demonstrate this, we phototransfected a modified HEK293 cell line, which expresses the newly identified gene termed willin/FRMD6[13] under the control of an antibiotic inducible promoter, with small interfering RNA (siRNA) against willin; thus specifically blocking the expression of the willin gene product. This represents the first time siRNA has been transfected into mammalian cells using a cw laser source.

2 Materials and Methods

2.1 *Violet Diode Photoporation System*

The laser source was a commercially available 405-nm diode laser (Toptica, IBEAM-405-1V1 with an $M^2 < 1.2$) with maximum power of 40 mW. The beam was magnified by the telescope consisting of lenses L1 and L2 (Fig. 1). A half-wave plate and a polarizing beamsplitter in tandem were used to attenuate the beam power. A dichroic mirror at 45 deg reflected the beam to the rear entrance pupil of a high-numerical-aperture (NA) water immersion, violet corrected microscope objective (Nikon Plan Apo; magnification=63× NA=1.20) with measured transmission of ~84% at 405 nm. The laser was focused to a diffraction-limited spot approximately 0.4 μm in diameter. The power at the sample plane was obtained by taking the power transmission measurements through the optics. The maximum laser power dosages for each cell were first characterized by empirically observing the cell for any signs of granulation, blebbing, or necrosis. A beam shutter (Newport, United Kingdom, model 845 HP-02) placed in front of the laser was used to control the exposure times. An exposure time of 1 s was used to observe the transfection efficiency for each power level employed. Bright-field illumination in Koehler configuration was used to illuminate the sample. The image plane and laser plane were made coincident by changing the positions of lenses L1 and L2 and observing the image and laser focus. An *xyz* stage enabled us to vary the sample position. Finally, a color CCD camera (WATEC 250D) was used to capture the videos of the process.

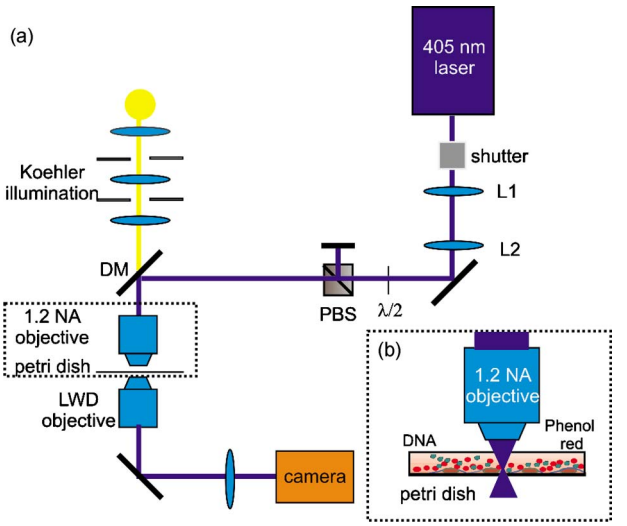

Fig. 1 (a) Schematic of a photoporation system using a 405-nm diode laser: L (L1=50 mm and L2=100 mm), plano-convex lenses; PBS, polarizing beamsplitter; M, mirrors; DM, dichroic mirror; and LWD, long-working-distance objective. The whole system is mounted on a 60×90 cm optical breadboard. (b) Schematic layout of a prepared sample in a petri dish showing the laser beam focused on a cell bathed in DNA and phenol red solution.

2.2 *Cell Culture Procedure*

CHO-K1 cells and HEK293 cells were cultured in T25 flasks at 37 °C and 5% CO_2 in modified Eagle's medium (Sigma, United Kingdom) with 10% fetal calf serum (GlobePharm, University of Surrey, United Kingdom), 20 μg/ml streptomycin (Sigma, United Kingdom), and 20 μg/ml penicillin (Sigma, United Kingdom).

A stable tetracycline inducible system, TRex willin-GFP-HEK, was created using a TRex inducible plasmid pcDNA4/TO/myc-his (Invitrogen, United Kingdom) modified to express willin-GFP, which was then transfected into stable HEK293 cells containing a plasmid expressing a tetracycline repressor, pcDNA6/TR. TRex willin-GFP-HEK cells were cultured in T25 flasks in the presence of Dulbeco modified Eagle's medium (Sigma, United Kingdom) with 10% fetal calf serum (GlobePharm, University of Surrey, United Kingdom), 2 mM L-glutamate, 100 units/ml penicillin and 100 units/ml streptomycin (Sigma, United Kingdom). Stable cells were selected by the addition with 5 μg/ml blasticidin and 250 μg/ml zeocin. Willin-GFP expression was induced with 1 μg/ml tetracycline (Invitrogen, United Kingdom).

Cells were routinely passaged three times a week. CHO-K1 and HEK293 cells were seeded at a density of 2.4×10^4 cells/ml onto 35-mm glass-bottomed culture grade dishes (World Precision Instruments) to achieve 40 to 50% confluency. The cells were incubated at 37 °C for 24 h to allow cell attachment to the bottom of the glass dishes. Meanwhile, TRex willin-GFP-HEK cells were plated 48 h prior to the experiment onto 35-mm culture dishes coated with laminin (Invitrogen, United Kingdom) to improve cells' adherence on the dishes.

2.3 *Targeted DNA Phototransfection*

For each phototransfection experiment, individual CHO-K1 and HEK293 cells were exposed to up to 3.4 mW of laser power for 1 s at the focus. Before exposure, the cell monolayer was washed twice with OptiMEM (Invitrogen, United Kingdom) and then bathed with 30 μl of solution containing 10 μg/ml plasmid encoding for Mito-DsRed (Clontech) and 42.2 μM of phenol red (Sigma) in OptiMEM. Phenol red is a dye commonly used with cell culture media to detect changes in pH. The absorption of the solution used in the photoporation experiments was measured and a molar coefficient cross section of $\sim1.4\times10^4$ cm^{-1} M^{-1} at 405 nm was obtained.

A type 0, 22-mm-diam coverslip was placed on top of the cell monolayer and a region of interest was marked in the center in order to identify the region of dosed cells. On average, 50 healthy looking cells per dish were irradiated on the plasma membrane in a region 1 to 3 μm away from (and not directly above) the nucleus. After dosage, the coverslip was removed with OptiMEM and phenol red solution, and then subsequently washed twice with the same medium. The cells were then further incubated in fresh medium for up to 72 h after photoporation. Control cells were prepared in the same manner but were not exposed to the laser. The photoporated cells were observed under a fluorescent microscope for expression of the Mito-DsRed gene. For each laser power and for each irradiation time, nine experiments were performed, irradiating 50 cells per dish in the process. Therefore in total, for $n=9$ experiments, ~5000 cells were treated, enabling us to accumulate reliable statistics of the process.

2.4 *Cell Viability*

HEK293 cells were plated on 35-mm glass-bottomed dishes and were prepared similarly to transfection experiments except no DNA was added. Cells were exposed to 2.1- and 3.4-mW laser power at exposure times from 80 ms to 5 s. After laser exposure, cells were returned in the incubator for an hour, after which 60 μl of 0.3% trypan blue was added. Trypan blue is an indicator of cell membrane barrier dysfunction. In the state of necrosis, the cell's protective membrane is often compromised, leading to intake of extracellular material. Dead cells stained blue were counted and the viability was calculated by obtaining the percentile ratio of dead cells with irradiated cells. Each data point was an average of three dishes and 50 cells per dish were exposed to the laser.

2.5 *siRNA Chemical Transfection*

Willin knockdown was performed using small interfering RNA (siRNA), to a final concentration of 5 nM, specifically targeting the protein (GACAGAGCAGCAAGAUACUAUUAUU, CACAGACUAUAUGUCGGAAACCAAA, GCCUCUAUAUGAAUCUGCAGCCUGU; Invitrogen) using Gene Eraser (Startagene) according to the manufacture's instructions. Protein expression was analyzed by Western blotting, using anti-GFP (Santa-Cruz) and anti-actin (Sigma) as a loading control.

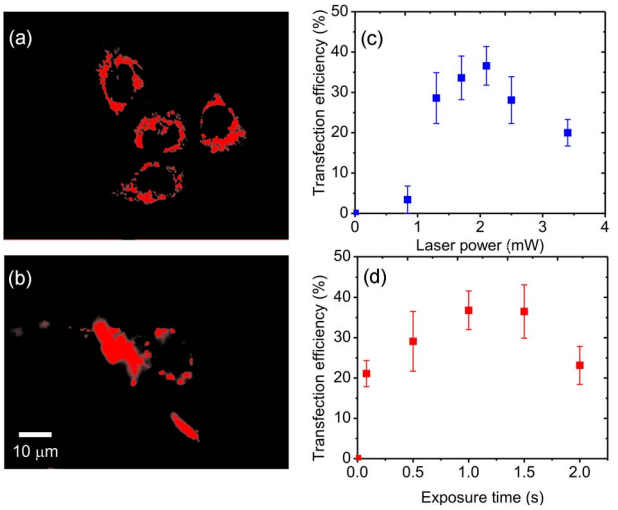

Fig. 2 Fluorescence images of transfected (a) CHO-K1 and (b) HEK293 transfected with Mito-DsRed plasmid, (c) transfection efficiency of HEK293 cells as a function of laser power at the focus using a 1-s exposure time, and (d) transfection efficiency of HEK293 cells as a function of laser exposure time at 2.1 mW. The error bars represent standard deviation, ($n=9$ experiments of 50 dosed cells).

2.6 *Fluorescence Microscopy*

All fluorescence microscopy was performed on a TE2000-E, Nikon microscope. Cells expressing Mito-DsRed were imaged using TRITC HYQ, Nikon Filter cube (excitation, 530 to 560 nm; emission, 590 to 650 nm). Meanwhile, cells induced and expressing willin-GFP were imaged using FITC HYQ Nikon filter cube (excitation, 460 to 500 nm; emission, 510 to 560 nm).

3 Results

3.1 *DNA Phototransfection*

Phototransfection experiments on CHO-K1 and HEK293 cells were performed using a violet diode laser. For the laser parameters used, and under bright-field imaging, no visible reaction from the cell was observed. Successful transient expression was achieved with the Mito-DsRed plasmid for both cell lines, as shown in Figs. 2(a) and 2(b). The transfection efficiency after 72 h as a function of laser power, using a 1-s exposure time for HEK293 cells, is shown in Fig. 2(c). Each power level is significantly different from the control group ($p<0.05$) with the exception of 0.8 mW, as determined by a one-way analysis of variance (ANOVA) followed by Dunnett's statistical test. Overall, a Poisson distribution curve was obtained where the start and tail of the plot were significantly different from each other, as determined from ANOVA followed by Fischer's pairwise test ($p<0.05$). As indicated in Fig. 2(c) an enhancement of transfection efficiency was acquired with an increase in laser power from 0.8 to 1.3 mW

with efficiencies of 3.4 ± 3.4 to $28.6 \pm 6.3\%$, respectively, typifying a power dependence on the probability of cell poration and subsequently transfection. The optimum laser power was found to range from 1.3 to 2.5 mW, which yielded transfection efficiencies between 28.1 ± 5.8 and $36.6 \pm 4.8\%$. Within this range of power levels, the efficiencies were not significantly different from each other but were significantly different from 0.8 and 3.4 mW ($p < 0.05$). Additionally, as the mitochondria were tagged, it was possible to observe their streaming, which is an indicator of the overall health of the treated cells. In comparison, the highest transfection efficiency for CHO-K1 was at $23 \pm 1.5\%$. As established previously,[1] the level of spontaneous transfection was very low and negligible in comparison to the transfection efficiencies we achieved. Spontaneous transfection is defined as cells expressing the protein without exposure to the laser irradiation.

The dependence of transfection efficiency on laser exposure time was also studied for a laser power of 2.1 mW for HEK293 cells. Figure 2(d) shows the transfection efficiency as a function of irradiation time from 80 ms to 2 s. An ANOVA followed by Dunnett's statistical test showed that transfection efficiencies obtained from different exposure times were significantly different compared to the control ($p < 0.05$). Though significant transfection efficiency can already be obtained at a 80-ms exposure, 1.0 and 1.5 s appeared to be optimal for transfection at this laser power. Increasing the exposure time from 1.5 to 2 s resulted in the decline of the average transfection efficiency from 36.5 ± 6.6 to $23 \pm 4.7\%$, respectively, which may be a consequence of a decrease in viability (see in the following).

3.2 *Phototoxicity of Violet Diode Phototransfection*

Careful assessment of the cell viability was performed by exposing the cells to the laser and monitoring any morphological changes in the cells. Cells exposed to 2.1 mW for 6 to 10 s immediately showed signs of necrosis. In a further study, the viability of the cells treated with the laser at shorter exposure times were measured for two laser powers, 2.1 and 3.4 mW, as shown in Fig. 3 (laser exposure ranged from 0.08 to 5 s) in the presence of trypan blue.

In general, viability was observed to decrease with increasing laser exposure time. For a 1-s exposure, viability was measured from 96.4 ± 1.2 and $95.4 \pm 1.2\%$ for laser powers of 2.1 and 3.4 mW, respectively. It marginally decreased from 86.7 ± 1.2 to $65.3 \pm 4.2\%$ at 2 s, respectively. This small increase in laser power from 2.1 to 3.4 mW resulted in a sixfold decline in viability at 3-s exposure times from 72 ± 9.2 to $11.3 \pm 12.1\%$. It was found that viability exponentially decays with exposure time and laser power. LD50, defined as dosage entailing 50% cell viability occurs at an energy density of ~ 6.3 MJ/cm^2.

Notably, with laser exposures beyond the therapeutic dosage for transfection, fluorescence was observed at the targeted site, an indication of single-photon absorption, which might lead to the melting of the plasma membrane. Often when this phenomenon occurred, the cell underwent blebbing, granulation, loss of intracellular material, and necrosis. Neighboring cells, however, were not affected.

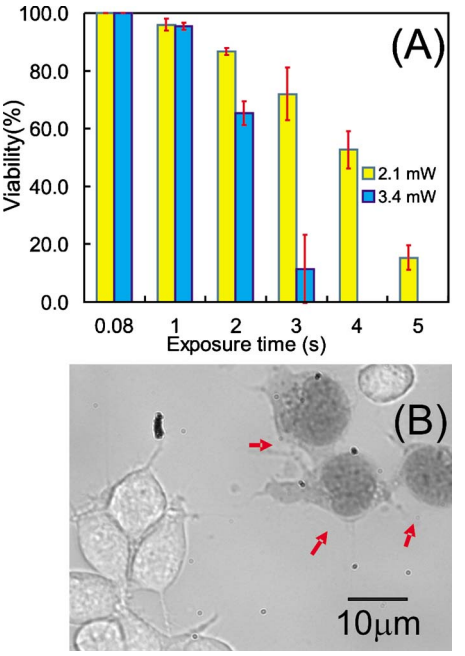

Fig. 3 (a) Viability of HEK293 cells exposed to laser at 2.1 and 3.4 mW at the focus at varying exposure time. Error bars represent ± standard deviation ($n = 3$ experiments of 50 dosed cells). (b) Bright-field image of laser exposed HEK293 cells. Cells pointed to by the red arrows were irradiated with the laser and have taken up the trypan blue dye, a sign of cellular necrosis. (Color online only.)

3.3 *Cell-Specific Gene Knockdown Experiments*

RNA interference (RNAi) is a technology developed by Fire et al.[14] in 1998 that enables the knockdown in expression of a specific gene. siRNA interferes with new protein expression, resulting in silencing of the gene. siRNA is made from a length of 20 to 25 nucleotides that bind specifically to the messenger RNA (mRNA) of the protein of interest. This leads to the formation of a siRNA complex, which results in mRNA cleavage and its subsequent degradation.[15] The applications of this widely used gene silencing technology include studying a gene's function, but also the potential therapeutic modification of gene expression in human diseases. Therefore, for the reasons outlined in the introduction, we explored the possible use of violet diode lasers in cell-specific gene knockdown experiments.

TRex willin-GFP-HEK cells were induced with 1 μg/ml tetracycline to activate willin-GFP expression. After 24 h, 5 nM siRNA manufactured to recognize specifically the willin gene, was chemically transfected into these cells. Willin-GFP protein levels were detected 24, 48, and 72 h after siRNA treatment. Western blot analysis (Fig. 4) shows that willin-GFP expression is significantly reduced after 48 to 72 h of siRNA transfection. Actin was used as a loading control and expression levels remain unchanged throughout siRNA transfection. This, therefore, indicated that the siRNA used were specific and effective in decreasing willin expression.

Therefore, for the photoporation experiments, 5 nM stock of the siRNA duplexes with the Mito-DsRed-encoding plasmid was added to the transfection medium. Initially, 10 μg/ml of Mito-DsRed was also added to identify cells

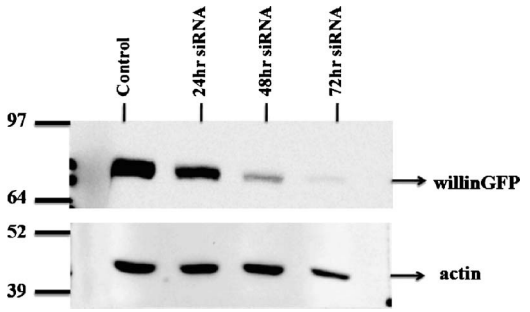

Fig. 4 Western blot analysis showing reduction of willin-GFP expression after 48 h of 5 nM siRNA chemical transfection. TRex willin-GFP cells were induced with 1 μg/ml tetracycline to express willin-GFP 24 h prior to siRNA treatment. Western blots were probed with anti-GFP and anti-actin, with the latter used as a loading control.

that had been successfully transfected. Cells were targeted using a 3.4-mW laser power at the focus and a 1-s exposure time. Control dishes included (1) cells with Mito-DsRed plasmid and the siRNA without laser treatment; (2) cells without the Mito-DsRed plasmid but with siRNA without laser treatment, and (3) cells without both the Mito-DsRed and siRNA with laser treatment. Expression of willin-GFP was then induced by the addition of tetracycline, and cells were monitored for fluorescence over the next 2 days. For all control dishes, spontaneous DNA transfection or knockdown was not observed.

Figure 5 shows images of photoporated TRex willin-GFP-HEK cells in the presence of the willin specific siRNA and the Mito-DsRed plasmid. Figure 5(a) is a successfully transfected TRex willin-GFP-HEK cell, as shown by the expression of mitochondrial targeted red fluorescent protein captured using the TRITC HYQ, Nikon Filter cube. Figure 5(b) is the same field of view but under bright-field imaging. Figure 5(c) shows the same cells, but imaged now using a FITC HYQ Nikon filter cube. As indicated by the blue and red arrows are cells that exhibit clear knocked down of willin-GFP expression, as indicated by the absence of green fluorescence. One cell, indicated by the red arrow point, was also transfected with the Mito-DsRed encoded plasmid. The laser's specificity of action is indicated by the fact that untreated cells have not been knockdowned or transfected with Mito-DsRed, as observed in all control dishes checked under a fluorescence microscope and confirmed by Western blot analysis (data not shown).

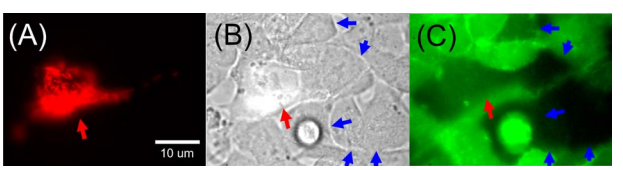

Fig. 5 Gene knockdown using a violet diode system. (a) A TRex-willin-GFP-HEK cell fluorescing red due to the expression of the Mito-DsRed and (b) under bright-field imaging; (c) fluorescence image of the same field of view using a FITC HYQ. The Red arrow points to a cell that has been cotransfected with Mito-DsRed and willin specific siRNA. Blue arrows point to cells that have been transfected with siRNA only. (Color online only.)

3.4 *Temperature Calculations at the Focal Volume*

Based on previous reports using the cw violet laser for transfection, it was conjectured that a melting of the phospholipid bilayer occurs due to the direct absorption of the phenol red in the medium, causing localized thermal effects on the irradiated site.[8,10] To elucidate the mechanistic process of poration, an estimate of the temperature at the beam focus was calculated based on modeling the phenol red as a sphere of radius r immersed in a nonabsorbing medium. Since the absorption and the consequential increase in temperature occur only in close proximity to the focus, one can assume that the laser energy is absorbed only by the phenol red sphere. The radius r of the sphere can be made equivalent to the radius of the beam spot given by $r=0.61\lambda/\mathrm{NA}$, where $\lambda=405$ nm and $\mathrm{NA}=1.2$.

Since most of the incident power of the laser goes through the sphere of radius r, we can assume that the substitution of focused Gaussian beam with a plane wave of incident intensity $I=P/(\pi r^2)\sim 1\times 10^{10}$ W/m^2, where P is the power of the laser at the focal plane going through the geometrical cross section of the sphere, will not introduce any significant error to our estimate. The Mie scattering problem can be solved for the phenol red sphere surrounded by the nonabsorbing medium. The imaginary part of the index of refraction of the phenol red sphere was determined by the equation $\hat{n}=n[1+i(\alpha\lambda/4\pi n)]$, based on the measured absorption coefficient, $\alpha=0.6$ cm^{-1}, noting that the change in the real part of the index of refraction n is negligible. This yielded an expression for the index of refraction given by $\hat{n}=1.33+i(1.93\times 10^{-6})$. The solution provides us the absorption cross section σ of the phenol red sphere, which is $\sigma=2\times 10^{-18}$ m^2. Hence, the heat absorbed Q by the phenol red can be obtained, where $Q=I\sigma\sim 3\times 10^{-8}$ W.

Since, the cw irradiation used for the experiments lasts of the order of milliseconds to seconds and the temperature change saturates immediately after several microseconds,[12] we modeled only the steady state temperature increase, ΔT which is given by $\Delta T=(1/4\pi)(Q/\kappa_0 r)$,[16] where $\kappa_0=0.6$ W/mK is the thermal conductivity of water. We assumed the same thermal conductivity for phenol red. From this, the calculated ΔT is 0.02 K.

4 Discussion

Femtosecond near-IR lasers are generally much more effective tools for cell nanosurgery compared to cw lasers due to the mechanisms of their interaction with biological material.[12] However, since both work with a tightly focused laser beam that is typically an order of magnitude smaller than the cell's diameter ($\sim$10 to 20 μm), they may both be suitable for single-cell transfections studies. In particular, the violet diode laser can be a compact and cost-effective biological transfection tool when compared to the use of a femtosecond pulsed laser.

In contrast to previous work,[8,10] which reported small dark circular spots on the cell that disappeared several minutes after laser irradiation, these dark spots were not observed during our experiments. More conclusively, these dark circular spots repeatedly appear for cells irradiated with laser parameters beyond a therapeutic dosage. No visible reaction, hole,

or cavitation bubble from the cell was observed using the laser and exposure times described in this paper for successful transfection. Whether DNA transfection necessitates a nanosize hole is not yet confirmed, but the increase in membrane permeability may be enough to allow a circular DNA plasmid to enter through the cell membrane. Further studies will be necessary to discover changes within the membrane structure at the site of laser irradiation.

In this work, transient transfection as opposed to stable transfection of CHO-K1 and HEK293 cells were achieved. Selection of cells with integrated DNA in their nuclear genome using an antibiotic called G418 was still also possible and thus enabled us to generate stable colonies from our transiently transfected cell lines. However, the laser energy used in this work was of the order of 2000 μJ, compared to only 12 μJ used by Paterson et al.[1] Successful transient transfection using our cw focused 405-nm laser required an energy density of 1.5 MJ/cm^2, in close agreement with the energy density reported using a focused 488-nm argon-ion laser ($\sim$1 MJ/cm^2).[10]

The cw cell poration was suggested to be mainly due to the large temperature rise in the absorptive medium leading to pore formation on the cell membrane[8,10] however, the temperature calculation at the focus in the phenol red medium reveals that the gradient temperature is very small $\sim$0.02 °C. Our experiments were performed at 25 °C. Hence, the calculated temperature change is insufficient to achieve the reported temperatures of 42 to 45 °C, which are necessary for a membrane phase transition,[17] and is certainly well short of the required temperature rise for microbubble formation.[12] This may imply that a photochemical reaction dominates during irradiation by a focused 405-nm laser related to affecting membrane integrity. Oxidative stress induced by the production of reactive oxygen species (ROS) such as O_2^-, OH*, and H_2O_2 radicals, is known to be elicited by the irradiation of light at this wavelength region,[18–21] which may lead to subsequent lipid peroxidation, closely related to possible impairment of the phospholipid bilayer.[22] At the site of irradiation, localized production of ROS may occur, leading to changes in membrane permeability. The fact that oxidative stress may be involved in this process would agree with our observations that the addition of phenol red enhanced the overall transfection efficiency. Presumably, because it has been previously shown that phenol red can protect against the harmful effects of ROS[23] but its presence in the medium will not inhibit the localized ROS generated at the site of irradiation. Experiments revealed that cell poration was dose dependent, varying as a function of both exposure time and average power. Future extensive experiments will be required to elucidate the exact mechanism for poration events caused by violet diode laser light.

Studies have shown that violet-blue light induces damage through absorption by cellular endogenous photosensitizers,[21,24] which subsequently leads to adverse chemical reactions. Possible cellular chromophores absorbing in the violet-blue region include porphyrin ring structures and flavins.[18–20] In addition, Hockberger et al.[20] reported induced damage by violet light (400 to 410 nm) from a xenon arc mercury lamp on mammalian cells due to stimulated production of H_2O_2 by photoreduction of flavins and/or flavins containing oxidases located within the mitochondria and peroxisomes. ROS production was also equivalently observed using near-IR femtosecond laser pulses, which they attribute to two-photon absorption.[25] Oxidative stress may lead to several structural deformations such as fragmentation and condensation of nuclei, DNA strand breaks, and loss of membrane protective functionality leading to cell apoptosis.[25] Despite this, we have shown that good viability $\sim$90% can still be obtained at optimal parameters with controlled power and exposure time of the focused violet diode laser.

Successful gene knockdown was also achieved using the violet diode laser. Interestingly, there were more occurrences of gene knockdown with the siRNA than with DNA transfection, as shown in Fig. 5(c), where five cells (blue arrows) had knockdown of willin-GFP expression but were not expressing Mito-DsRed. It can be deduced that the efficiency for gene knockdown will be higher compared to DNA transfection as siRNA are much smaller compared to DNA plasmids [i.e., 25 bp (base pairs) versus $\sim$5000 to 6000 bp]. Assuming passive diffusion of DNA or siRNA from an extracellular medium to cytosol during phototransfection, one could compare the rate of diffusion of plasmid DNA and siRNA. The diffusion coefficient could be obtained using the equation $D=(kT/6\pi\eta R_G)$, where k is Boltzmann's constant, η is the viscosity of the medium, and T is the temperature in kelvin.[26] For siRNA, the Flory scaling law could apply, and the radius of gyration R_G is given by $R_G=5.5N^{1/3}$, where N is the number of base pairs.[27] Meanwhile, an estimated relation of R_G based on N for supercoiled DNA plasmids has was derived by Prazeres, where $R_G=0.402\times N$.[28] Based on these relations, we approximated that the 25-bp siRNA diffuses approximately 100× faster than a 5600-bp plasmid DNA, enabling more siRNA molecules to diffuse into the irradiated site than plasmid DNA.

In conclusion, transient transfection of mammalian cells using a violet diode laser was demonstrated. Our studies pave the way for a compact, miniature system utilizing low-power diode systems for cell transfection, which would make it inexpensive and accessible. We also showed that cell-specific gene knockdown experiments are possible with photoporation, opening up new vistas in cell biology. Notably, this is the first technique that would enable the knockdown of a specific gene in a specific cell while it is surrounded by other cells. Such technology would be of particular interest to cell biologists exploring cellular behavior in multicellular tissue.

Acknowledgments

We thank Dr. David Stevenson for useful discussions. We thank the United Kingdom Engineering and Physical Sciences Research Council and Biotechnology and Biological Sciences Research Council for funding. MLT acknowledges the support of a SUPA Prize Studentship. KD is a Royal Society-Wolfson Merit Award Holder. FGM and KD contributed equally to this work.

References

1. L. Paterson, B. Agate, M. Comrie, R. Ferguson, T. K. Lake, J. E. Morris, A. E. Carruthers, C. T. A. Brown, W. Sibbett, P. E. Bryant, F. Gunn-Moore, A. C. Riches, and K. Dholakia, "Photoporation and cell transfection using a violet diode laser," *Opt. Express* **13**(2), 595–600 (2005).

2. D. Stevenson, B. Agate, X. Tsampoula, P. Fischer, C. T. A. Brown, W. Sibbett, A. Riches, F. Gunn-Moore, and K. Dholakia, "Femtosecond optical transfection of cells: viability and efficiency," *Opt. Express* **14**(16), 7125–7133 (2006).
3. X. Tsampoula, V. Garces-Chavez, M. Comrie, D. J. Stevenson, B. Agate, C. T. A. Brown, F. Gunn-Moore, and K. Dholakia, "Femtosecond cellular transfection using a nondiffracting light beam," *Appl. Phys. Lett.* **91**(5), 053902–053903 (2007).
4. L. E. Barrett, J. Y. Sul, H. Takano, E. J. Van Bockstaele, P. G. Haydon, and J. H. Eberwine, "Region-directed phototransfection reveals the functional significance of a dendritically synthesized transcription factor," *Nat. Methods* **3**(6), 455–460 (2006).
5. C. McDougall, D. J. Stevenson, C. T. A. Brown, F. Gunn-Moore, and K. Dholakia, "Targeted optical injection of gold nanoparticles into single mammalian cells," *J. Biophoton.* **2**(12), 736–743 (2009).
6. I. B. Clark, E. G. Hanania, J. Stevens, M. Gallina, A. Fieck, R. Brandes, B. O. Palsson, and M. R. Koller, "Optoinjection for efficient targeted delivery of a broad range of compounds and macromolecules into diverse cell types," *J. Biomed. Opt.* **11**(1), 014034 (2006).
7. W. Tao, J. Wilkinson, E. J. Stanbridge, and M. W. Berns, "Direct gene-transfer into human cultured-cells facilitated by laser microPuncture of the cell-membrane," *Proc. Natl. Acad. Sci. U.S.A.* **84**(12), 4180–4184 (1987).
8. G. Palumbo, M. Caruso, E. Crescenzi, M. F. Tecce, G. Roberti, and A. Colasanti, "Targeted gene transfer in eucaryotic cells by dye-assisted laser optoporation," *J. Photochem. Photobiol., B* **36**(1), 41–46 (1996).
9. A. V. Nikolskaya, V. P. Nikolski, and I. R. Efimov, "Gene printer: laser-scanning targeted transfection of cultured cardiac neonatal rat cells," *Cell Adhes Commun.* **13**(4), 217–222 (2006).
10. H. Schneckenburger, A. Hendinger, R. Sailer, W. S. L. Strauss, and M. Schmidtt, "Laser-assisted optoporation of single cells," *J. Biomed. Opt.* **7**(3), 410–416 (2002).
11. U. K. Tirlapur and K. Konig, "Targeted transfection by femtosecond laser," *Nature* **418**(6895), 290–291 (2002).
12. A. Vogel, J. Noack, G. Huttmann, and G. Paultauf, "Mechanisms of femtosecond laser nanosurgery of cells and tissues," *Appl. Phys. B: Lasers Opt.* **81**, 1015–1047 (2005).
13. F. J. Gunn-Moore, G. I. Welsh, L. R. Herron, F. Brannigan, K. Venkateswarlu, S. Gillespie, M. Brandwein-Gensler, R. Madan, J. M. Tavaré, P. J. Brophy, M. B. Prystowsky, and S. Guild, "A novel 4.1 ezrin radixin moesin (FERM)-containing protein, 'Willin,'" *FEBS Lett.* **579**(22), 5089–5094 (2005).
14. A. Fire, S. Xu, M. K. Montgomery, S. A. Kostas, S. E. Driver, and C. C. Mello, "Potent and specific genetic interference by double-stranded RNA in *Caenorhabditis elegans*," *Nature* **391**(6669), 806–811 (1998).
15. M. T. McManus and P. A. Sharp, "Gene silencing in mammals by small interfering RNAs," *Nat. Rev. Genet.* **3**(10), 737–747 (2002).
16. G. Baffou, R. Quidant, and C. Girard, "Heat generation in plasmonic nanostructures: influence of morphology," *Appl. Phys. Lett.* **94**(15), 153109 (2009).
17. J. R. Dynlacht and M. H. Fox, "Heat-induced changes in the membrane fluidity of Chinese hamster ovary cells measured by flow cytometry," *Radiat. Res.* **130**(1), 48–54 (1992).
18. J. B. Lewis, J. C. Wataha, R. L. W. Messer, G. B. Caughman, T. Yamamoto, and S. D. Hsu, "Blue light differentially alters cellular redox properties," *Gold Bull.* **72B**(2), 223–229 (2005).
19. M. Eichler, R. Lavi, A. Shainberg, and R. Lubart, "Flavins are source of visible-light-induced free radical formation in cells," *Lasers Surg. Med.* **37**(4), 314–319 (2005).
20. P. E. Hockberger, T. A. Skimina, V. E. Centonze, C. Lavin, S. Chu, S. Dadras, J. K. Reddy, and J. G. White, "Activation of flavin-containing oxidases underlies light-induced production of H_2O_2 in mammalian cells," *Proc. Natl. Acad. Sci. U.S.A.* **96**, 6255–6260 (1999).
21. M. L. Cunningham, J. S. Johnson, S. M. Giovanazzi, and M. J. Peak, "Photosensitized production of superoxide anion by monochromatic (290–405 nm) ultraviolet irradiation of NADH and NADPH coenzymes," *Photochem. Photobiol.* **42**(2), 125–128 (1985).
22. P. Morlière, A. Moysan, R. Santus, G. Hüppe, J.-C. Mazière, and L. Dubertret, "UVA-induced lipid peroxidation in cultured human fibroblasts," *Biochim. Biophys. Acta Lipids and Lipid Metab.* **1084**(3), 261–268 (1991).
23. A. Grzelak, B. Rychlik, and G. Bartosz, "Light-dependent generation of reactive oxygen species in cell culture media," *Faraday Symp. Chem. Soc.* **30**(12), 1418–1425 (2001).
24. C. Kielbassa, L. Roza, and B. Epe, "Wavelength dependence of oxidative DNA damage induced by UV and visible light," *Carcinogenesis* **18**(4), 811–816 (1997).
25. U. K. Tirlapur, K. Konig, C. Peuckert, R. Krieg, and K. J. Halbhuber, "Femtosecond near-infrared laser pulses elicit generation of reactive oxygen species in mammalian cells leading to apoptosis-like death," *Exp. Cell Res.* **263**(1), 88–97 (2001).
26. K. Ribbeck and D. Gorlich, "Kinetic analysis of translocation through nuclear pore complexes," *EMBO J.* **20**(6), 1320–1330 (2001).
27. C. Hyeon, R. I. Dima, and D. Thirumalai, "Size, shape, and flexibility of RNA structures," *J. Chem. Phys.* **125**(19), 194905 (2006).
28. D. M. F. Prazeres, "Prediction of diffusion coefficients of plasmids," *Biosens. Bioelectron.* **99**(4), 1040–1044 (2008).